

## EXPERIMENTAL AND ANALYTICAL STUDY OF STRENGTHENED REINFORCED REACTIVE POWDER CONCRETE EDGE BEAMS UNDER COMBINED LOADING

ASHRAF A. ALFEEHAN<sup>1,\*</sup>, RANA H. ALKERWEI<sup>2</sup>

<sup>1</sup>Civil Engineering Department, College of Engineering,  
Mustansiriyah University, Baghdad, Iraq

<sup>2</sup>Highway and Transportation Engineering Department,  
College of Engineering, Mustansiriyah University, Baghdad, Iraq

\*Corresponding Author: drce\_ashrafalfeehan@uomustansiriyah.edu.iq

### Abstract

The interaction between the floor and the spandrel beam is subjected to a combined stress distribution induced by the effect of torsion, bending moment, and shear force make the load case more complicated. This study presents an investigation into the behaviour of nine RPC edge beams strengthened by CFRP fabric under torsional, flexural, and shear effects. The study aimed to verify the test method by comparing the experimental and analytical results to predict the RPC beam strength under a combined load. The experimental parameters included the transverse to longitudinal steel reinforcement ratio and the strengthening of the beam with transverse and longitudinal CFRP wrap. The combined load was applied by a manufactured steel arm to obtain the effect of torsion, bending, and shear forces simultaneously. Analytical calculations were made based on equations of torsion, flexure, and shear strengths presented in previous studies. The results showed that the experimental torsional strength of the RPC edge beam increased when the longitudinal reinforcement increased with a constant of the shear reinforcement regardless of the CFRP effect. Unlike the analytical results, the experimental results revealed that the longitudinal CFRP wrap improved the torsional capacity and this improvement increased as the longitudinal reinforcement increased. Also, the transverse CFRP wrap has a significant effect on the experimental torsional strength than the longitudinal CFRP. In all beams, the failure mode has occurred as a torsional failure mode without debonding the CFRP wraps. The experimental and analytical results showed acceptable agreement.

Keywords: CFRP, Edge beams, Reactive powder concrete, Strengthening, Torsion.

## 1. Introduction

Curved structural members in horizontal plan, eccentrically loaded beams, curved box girders in bridges and spandrel beams in buildings are typical examples of the structural elements subjected to torsional moments. Bending moments and shearing forces are usually associated with torsion, and the interaction among these loads is very important.

Torsion appears frequently in many structures especially in bridges, but rarely, pure torsion occurs alone in the structure. Most of the rehabilitation and repair studies are limited to pure flexural failure [1-6], shear failure [7-13], or both analytically and experimentally [14-18]. On the other hand, there are considerable studies that are conducted to understand the effect of flexural and shear [19-23], flexural and torsion [24-26] as well torsion [26-29], but combining the effect of flexural, shear and torsion have hardly been found. Strengthening or upgrading is necessary when the structural elements discontinue providing satisfactory strength and serviceability. In many applications for reasons like low weight, high strength, and durability; fibre-reinforced polymers FRP have been used successfully.

Much attention has been paid by many researchers to strengthen the reinforced concrete RC rectangular or double flange beams bonded with FRP for flexural and shear by experimental and numerical studies [30-34] while the need for research in the behaviour of beams strengthened with FRP under combined loading is still required. The investigations show that the ductility and torsional strength of the strengthened RC rectangular beams with FRP were reasonably increased [35, 36]. Hii and Al-Mahaidi [37] proposed a design tool to analyse the full torsional capacity of strengthened reinforced concrete beams that were validated against the experimental database. Ameli and Ronagh [38] introduced an analytical method for the evaluation of the torsional capacity of FRP strengthened RC beams.

Kwahk et al. [39] proposed a study to predict a formula for the torsional strength enabling to reflect the tensile strength of ultra-high-performance concrete UHPC beams based upon the thin-walled tube theory. The focus of this research is to investigate experimentally and analytically the strength of reactive powder concrete RPC edge beams strengthened with carbon fibre-reinforced polymers CFRP wrap under combined loading. Design codes such as ACI-318 do not provide the provisions for the torsional-flexural design of RPC beams thus a need exists to investigate the strength of RPC concrete in torsion-bending-shear interaction. The comparison of the ultimate strength calculated from equations proposed by other researchers with those observed in the experimental test is achieved in the present study. The analytical study is important in estimating and calculating the design loads of the RPC edge beams strengthened by CFRP under the combined loads. The study aims to verify the test method, compare the experimental and analytical results to predict the RPC beam strength, and evaluate the contribution of CFRP to beam strength.

## 2. Materials

Portland cement Type I from Tasluja Cement Company, in Sulaymaniyah and very fine sand passed on 600  $\mu\text{m}$  sieve from Al-Ukhaidir quarry in the western desert of Iraq were used in this work. A pozzolanic mineral admixture silica fume was added to the RPC mix as secondary cementitious material. A high-efficiency polycarboxylate polymer superplasticizer BETONAC-1030 from Leycochem

LEYDE Company in Iraq was also used in RPC mix. Micro stainless steel straight fibres copper-coated were used to reinforce the reactive powder slurry.

The properties of steel fibres, unidirectional CFRP fabric laminates and epoxy adhesive are listed in Table 1. The average yield stress and ultimate stress of the steel bars used are (510 and 720 MPa) respectively. The quantities of materials components of RPC mixture and test specifications are summarized in Table 2. Table 3 shows the results of the mechanical properties of control specimens according to the test specifications.

**Table 1. Properties of steel fibres, CFRP laminates and epoxy adhesive (according to the manufacturer's datasheet).**

Property	Steel fibres	CFRP Sika wrap 230 C/45	Epoxy resin Sikadur 330
Tensile strength MPa	2600	4300	30
Modulus of elasticity GPa	210	238	-
Flexural modulus MPa	-	-	3800
Tensile modulus MPa	-	-	4500
Thickness mm	0.22 (Dia.)	0.131	-
Length mm	13 (Straight)	Roll	-
Elongation at break %	-	1.8	0.9
Weight	-	230 g/m <sup>2</sup>	-
Density kg/m <sup>3</sup>	7800	-	-

**Table 2. Quantities of materials per cubic meter and test specifications.**

Material	Quantity kg	Test specification
Cement	1000	IQS No. 5 [40]
Sand	1000	IQS No. 45 [41]
Silica fume (8% of cement weight)	80	ASTM C1240 [42]
Water (w/c=0.25)	250	Tap water
Superplasticizer <sup>a</sup> (6% of cement and silica weight)	64.8	According to the manufacturer
Steel fibre (1% of total volume)	78	According to the manufacturer

<sup>a</sup>Density= 1.1 kg/L

**Table 3. Mechanical properties of RPC control specimens.**

Property	Number	Dimensions (mm)	Test specification	Test result (MPa)
Compressive strength ( $f_c$ )	3 Cylinders	300×150	ASTM C39 [43]	70.3
Splitting strength ( $f_{ct}$ )	3 Cylinders	300×150	ASTM C496 [44]	8.59
Modulus of rupture ( $f_r$ )	3 Prisms	500×100×100	ASTM C78 [45]	10.56
Modulus of elasticity ( $E_c$ )	3 Cylinders	300×150	ASTM C469 [46]	41530

The silica is mixed with cement firstly until the mixture is homogeneous, then fine sand is added till the mixture becomes one colour. After that, a solution of the

plasticizer and the required water is added progressively while mixing continues for a sufficient time to achieve reasonable fluidity. After the mixture is homogeneous and becomes semi-liquid, steel fibres are added during the mixing process gradually to prevent the occurrence of balling and accumulation. The specimens are vibrated, removed from the moulds after 48 hours, and then treated with water for 28 days.

### 3. Experimental Work

The experimental work included cast nine-edge RPC beams of L-section strengthened with CFRP fabric laminates. The edge beams were tested under combined load up to the point of failure. The combined load was applied by a device designed for this purpose. Load increments and crack propagation were monitored and recorded to determine the ultimate loads and modes of failure. The CFRP wrap was conducted in two directions; longitudinal on both web sides of the beam and transverse as U wrapping for the web and the bottom surfaces of the beam. Each web was strengthened by two parallel longitudinal CFRP strips of (30) mm width at a clear spacing of (40) mm. The U wrapping strengthening was by nine CFRP strips of (30) mm width at a clear spacing of (85) mm along the length of the beam.

The transverse and longitudinal CFRP were placed on the centres matched with the stirrups and longitudinal steel respectively. The area of longitudinal CFRP was 60% of the beam side, so no CFRP strip was placed on the mid-side to avoid full wrap. Three groups involved nine (L) edge beams with a length of (1000) mm was cast and tested up to the failure. The main parameters adopted in this work were the ratio of transverse to longitudinal reinforcing steel and the longitudinal and transverse strengthening by CFRP wrap. Figure 1 illustrates the distribution of the steel reinforcement in the beams. Two beams from each group were strengthened with CFRP wrap; one of them in the longitudinal direction and the other in the transverse direction. The Sikadur (330) epoxy resin is the adhesive glue used to paste the CFRP wrap on the concrete surface. Figure 2 shows the distribution of CFRP and the dimensions of the edge beam. The reinforcement and beam designation details are shown in Table 4. The beams were tested as cantilever beams with fixed support from one end and free from the other end. The fixed end of the beam was held by the press of the universal load test apparatus to achieve the fixed support condition.

To provide a combination of shear, bending and torsion forces, the load was applied on the free end of the RPC beam by a manufactured torque steel arm connected by a load cell and hydraulic jack. The section of the steel torque arm is a rectangular tube section with outer dimensions of (90 by 50 mm) and (5 mm) thickness. The flexural stiffness of the torque arm is much enough to transform the forces without bending deformation. The capacities of the hydraulic jack and the load cell used are (10 and 5 tons) respectively. The load cell has two threaded holes one at each end. The load cell connects from one of the end holes by a steel screw that welded on the head of the hydraulic jack. The other end hole of the load cell connects by another steel threaded rod. Three steel nuts were welded together to construct a threaded tube to fasten the load cell with the ball and socket part. The ball and socket welded to the torque steel arm to ensure that the applied load is to be always vertical to the torque arm during the stages of the loading. The loading system apparatus is illustrated in Fig. 3 and the beam under the loading system is shown in Fig. 4.

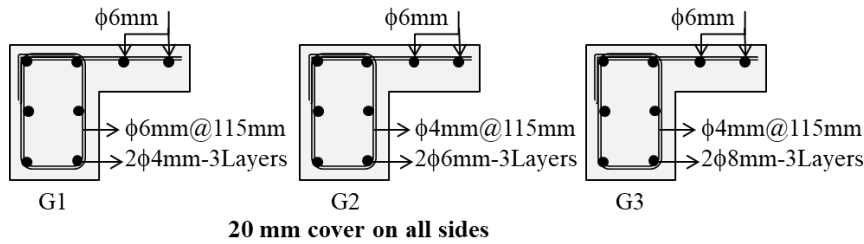


Fig. 1. Steel reinforcement details.

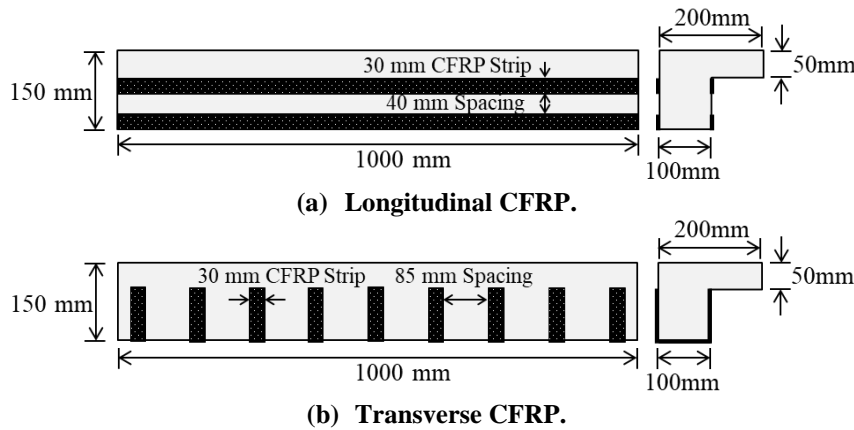


Fig. 2. Distribution of CFRP on the beam surface.

Table 4. Beam coding and experimental parameters details.

Group	Beam coding <sup>a</sup>	(T/L) Steel ratio <sup>b</sup>	CFRP wrap <sup>c</sup> (30 mm)	Bar diameter (mm)
G1	B <sub>1</sub> -4-6	0.58	-	φ4 in L, φ6 in T
	B <sub>1</sub> -4-6-CL		4-CL	
	B <sub>1</sub> -4-6-CT		9-CT	
G2	B <sub>2</sub> -6-4	0.15	-	φ6 in L, φ4 in T
	B <sub>2</sub> -6-4-CL		4-CL	
	B <sub>2</sub> -6-4-CT		9-CT	
G3	B <sub>3</sub> -8-4	0.095	-	φ8 in L, φ4 in T
	B <sub>3</sub> -8-4-CL		4-CL	
	B <sub>3</sub> -8-4-CT		9-CT	

Subscript number: Group number; L: Longitudinal direction; T: Transverse direction; C: CFRP wrap

- The first number refers to the diameter of the longitudinal steel bars, while the second number refers to the diameter of the transverse steel bars.
- Steel ratio = steel reinforcement ratio in transverse direction ( $A_{st}/(1000b)$ )/steel reinforcement ratio in longitudinal direction ( $A_{sl}/bh$ ), where  $b=100$  mm and  $h=150$  mm.
- The number in the CFRP wrap refers to the total number of CFRP wrap on the web of the beam; the letters CL and CT mean the presence of CFRP wrap in the longitudinal and transverse direction respectively.

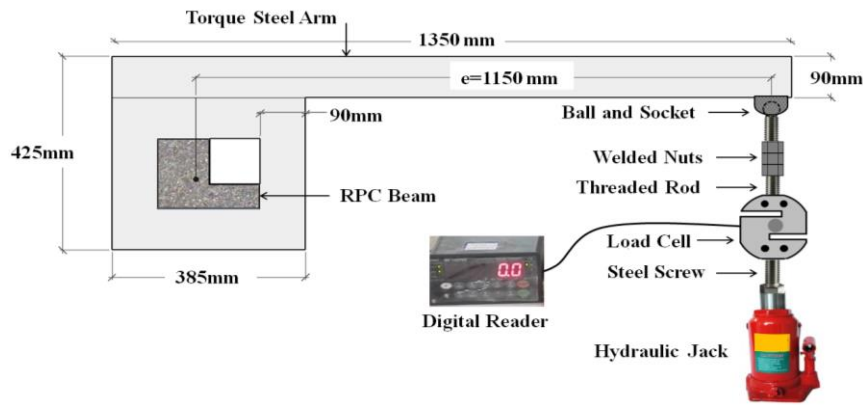


Fig. 3. Loading system.



Fig. 4. Beam under the loading system.

#### 4. Analytical study

The present work adopted the following equations proposed in previous studies to determine the torsional, shear, and flexural strengths for RPC beam strengthening by CFRP wrap. These equations were applied in this investigation to compare the analytical results with the results obtained from the experimental work:

##### 4.1. Torsional strength

The equation of Rahal [47] was used to calculate the torsional strength of RPC beams. This equation was proposed for the calculation of the ultimate torsional moment for the normal and high-strength concrete beams.

$$T_n = 0.33(f'_c)^{0.16} A_c (A_L f_{yL} \frac{A_t f_{yt}}{s})^{0.35} \leq 2.5(f'_c)^{0.3} \frac{A_c^2}{P_c} \quad (1)$$

There are many methods to calculate the contribution of CFRP in the torsional strength of the beams. In this study, the FIB-14 method proposed by Mohammadizadeh and Fadaee [48] was used.

$$T_{n_{frp}} = \epsilon_{ke,f} E_f \frac{t_f W_f}{s_f} A_c [\cot \alpha + \cot \beta] \sin \beta \quad (2)$$

$$\varepsilon_{ke,f} = \min \left[ \begin{array}{l} 0.8 * 0.65 \left( \frac{f_c^{\frac{2}{3}}}{\rho_f E_f} \right)^{0.65} * 10^{-3} \\ 0.8 * 0.17 \left( \frac{f_c^{\frac{2}{3}}}{\rho_f E_f} \right)^{0.3} \varepsilon_{fu} \end{array} \right] \leq \varepsilon_{max} = 0.005 \quad (3)$$

$$\rho_f = \frac{2t_f w_f}{b_w s_f} \quad (4)$$

### 4.2. Shear strength

The theoretical shear strength of the RPC beams was calculated by using the ACI Committee 440.2R [49] equations. The contributions of concrete, internal reinforcing steel and external CFRP wrap were considered in the nominal shear equation.

$$V_n = V_c + V_s + V_f \quad (5)$$

The concrete contribution was found using Ashour et al. [50] equation. Ashour et al. represented the ultimate shear strength of high strength fibre reinforced concrete beams for  $a/d \geq 2.5$ .

$$V_c = [2.11(f_c')^{0.33} + 7F] \left( \frac{\rho_w d}{a} \right)^{0.333} b_w d \quad (6)$$

$$F = \left( \frac{l_f}{d_f} \right) v_f B_f \quad (7)$$

The steel contribution is calculated by:

$$V_s = \frac{A_v f_y d}{s} \quad (8)$$

The ACI design guidelines for strengthening RC beams in shear with CFRP are based on empirical design equations derived by Triantafillou and Antonopoulos [30]. Shear contribution  $V_f$  of CFRP was found using Triantafillou equation.

$$V_f = \rho_f E_f \varepsilon_{ke,f} b_w z_f (1 + \cot \beta) \sin \beta \quad (9)$$

### 4.3. Flexural strength

The flexural strength of reactive powder concrete beam was found using Henager and Doherty equation which was adopted by the ACI-544 committee [51].

$$M_n = A_s f_y \left( d - \frac{a}{2} \right) + \sigma_t b (h - e) \left( \frac{h}{2} + \frac{e}{2} - \frac{a}{2} \right) \quad (10)$$

$$\sigma_t = 0.00772 \frac{l_f}{d_f} \rho_f F_{be} \quad (11)$$

$$\varepsilon_{sf} = \frac{\sigma_{sf}}{E_{sf}} \quad (12)$$

$$e = (\varepsilon_{sf} + 0.003) \left( \frac{c}{0.003} \right) \quad (13)$$

As a numerical case for a cantilever beam of length equals (1m), the torsion, shear, and flexure strengths were calculated according to the following equations. All numerical values required to apply the equations are given in Table 5.

$$\text{Torsion: } T_{theo} = \frac{T_n + T_{frpn}}{e}$$

Shear:  $S_{theo} = V_n$ Flexure:  $F_{theo} = M_n$ **Table 5. Numerical values of the applied equations.**

Symbol	Numerical value	Symbol	Numerical value	Symbol	Numerical value
$A_c$	15000 mm <sup>2</sup>	$d_f$	0.22 mm	$t_f$	0.131 mm
$A_L$	G1: 75.4 mm <sup>2</sup> G2: 169.2 mm <sup>2</sup> G3: 301.6 mm <sup>2</sup>	$E_f$	227000 MPa	$v_f$	0.01
$A_t$	G1: 28.2 mm <sup>2</sup> G2: 12.5 mm <sup>2</sup> G3: 12.5 mm <sup>2</sup>	$e$	1150 mm	$w_f$	30 mm
$A_v$	G1: 56.5 mm <sup>2</sup> G2: 25.1 mm <sup>2</sup> G3: 25.1 mm <sup>2</sup>	$F_{be}$	1	$Z_f$	G1: 98 G2: 97 G3: 96
$\underline{a}$	1000	$f'_c$	70.3 MPa	$\alpha$	45°
$B_f$	0.5	$l_f$	13 mm	$\beta$	90°(transverse) 0 (longitudinal)
$b_w$	100 mm	$S$	115 mm	$\rho_f$	0.01
$d$	G1: 123 mm G2: 122 mm G3: 121 mm	$S_f$	85 mm	$\rho_w$	G1: 0.002 G2: 0.0046 G3: 0.0083

## 5. Results and Discussion

The loads recorded from the experimental test, modes of failure, analytically calculated values of torsion, shear and flexural strength based on the transverse to longitudinal steel ratios and effect of CFRP were illustrated in Table 6. It is evident from the results that the experimental ultimate loads were close to the torsional strength of the analytical values. This means that the RPC beams first failed under the torsion effect. Also, the failure mode confirms that the RPC beams failed due to the shear stress result from the torsional force, as shown in Fig. 5. Diagonal cracks appeared on the perimeter of the beam section gradually. As the load increased, the cracks began to spread and expand until the failure occurred.

**Table 6. Experimental and theoretical failure loads.**

Beam Coding	(T/L) Steel ratio	$P_u^{Exp.}$ kN	$T_{Anal.}^a$ kN	$S_{Anal.}^b$ kN	$F_{Anal.}^c$ kN	Mode of Failure	$P_u^{exp./T_{Anal.}}$
B <sub>1</sub> -4-6	0.58	1.51	1.85	47.18	3.13	Torsional	0.81
B <sub>2</sub> -6-4	0.15	1.54	1.85	35	6.88	Torsional	0.83
B <sub>3</sub> -8-4	0.095	2.37	2.26	39.2	11.9	Torsional	1.04
B <sub>1</sub> -4-6-CL	0.58	1.55	1.85	47.18	3.13	Torsional	0.83
B <sub>2</sub> -6-4-CL	0.15	1.6	1.85	35	6.88	Torsional	0.86
B <sub>3</sub> -8-4-CL	0.095	3.1	2.26	39.2	11.9	Torsional	1.37
B <sub>1</sub> -4-6-CT	0.58	2.15	2.46	57.68	3.13	Torsional	0.87
B <sub>2</sub> -6-4-CT	0.15	2.28	2.46	45.39	6.88	Torsional	0.92
B <sub>3</sub> -8-4-CT	0.095	3.24	2.87	49.48	11.9	Torsional	1.12

<sup>a</sup> Based on Rahal [47] and Mohammadzadeh and Fadaee [48]

<sup>b</sup> Based on Triantafillou and Antonopoulos [30]

<sup>c</sup> Based on American Concrete Institute Committee 544 [49]





**Fig. 5. Failure mode pattern of the RPC beams.**

### **5.1. Effect of transverse to longitudinal reinforcement ratio**

It is important to know that the torsional strength calculated from the analytical equations depends on the product of  $(A_L \cdot A_t)$ . Therefore, the experimental comparison between the RPC beams becomes clearer based on the effect of this factor. The results showed that the experimental ultimate load of the RPC beams without, with longitudinal and with transverse CFRP increased by (2%, 3.2% and 6%) respectively when the  $T/L$  decreased from (0.58) to (0.15).

These increases are not significant when compared to the increase in the experimental ultimate load if  $(A_L \cdot A_t)$  increases to a higher value. In beam  $B_3$ , when the  $T/L$  decreased to (0.095) with a constant value of shear reinforcement compared to beam  $B_2$ , the experimental ultimate load increased by (54%, 93% and 42%) for the RPC beams without, with longitudinal and with transverse CFRP respectively. It was noted a significant increase in the beam strength by increasing the longitudinal reinforcement with constant transverse reinforcement and it was higher with the presence of the longitudinal CFRP.

The analytical shear strength is affected by  $(A_v)$  and  $(d)$ . For beams  $B_2$ , the shear strength decreased due to a decrease in the  $(A_v)$  while increased for beams  $B_3$  due to the increase of  $(d)$  with a constant value of  $(A_v)$ . It is also evident that the bending strength obtained from the equations increases with increasing the effective beam depth. The study showed that there was an agreement between the experimental and analytical results, which indicates that the test method was suitable to investigate the strength of RPC edge beam under combined loading. Figure 6 shows the effect of the ratio of the transverse to the longitudinal reinforcement on the experimental ultimate load.

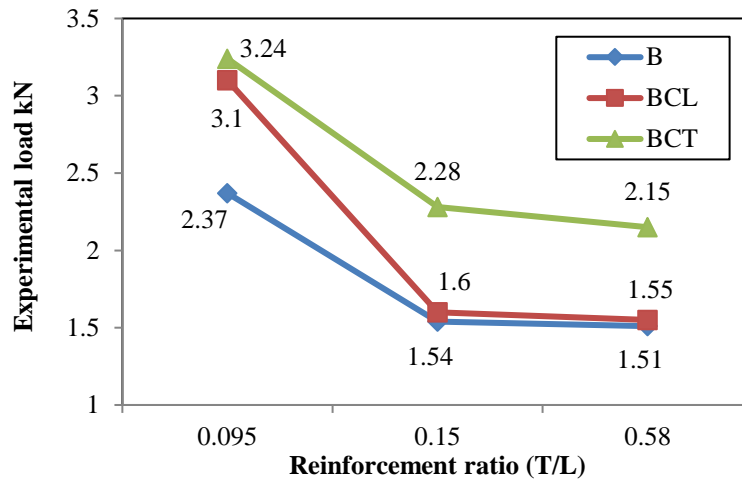


**Fig. 6. Effect of transverse to longitudinal steel reinforcement ratio on the experimental ultimate load.**

### 5.2. Effect of longitudinal CFRP

A slight increase occurred in the experimental ultimate load in the presence of the longitudinal CFRP when the  $T/L$  decreased from (0.58) to (0.15), while an increase of (30%) occurred when the  $T/L$  decreased to (0.095). The contribution of the longitudinal CFRP to the torsional strength disappeared in the analytical equations even with a change of  $(A_L, A_t)$ . The analytical torsional strength depends on the orientation CFRP angle which appears in  $(\sin\beta)$ . This term is equal to zero when the orientation angle ( $\beta$ ) of the horizontal CFRP is equal to zero. The design of torsion is based on a thin-walled tube space truss analogy in which, the strength is provided by the outer skin of the cross-section. As long as the longitudinal CFRP is placed on an area of (60%) (two strips of 30 mm each) of the side surface, the CFRP participation in increase the strength was by delaying the appearance of torsional cracks on the beam surface, even if it is in a longitudinal direction. After the RPC beam has cracked in torsion, the torsional strength is provided primarily by closed stirrups and longitudinal bars located near the surface. Due to its location on the surface, the CFRP starts first or coincides with RPC to withstand the torsional forces.

### 5.3. Effect of transverse CFRP

The transverse CFRP wrap had a larger effect on the ultimate load when the  $T/L$  steel ratio was the minimum. The experimental results showed that the transverse CFRP wrap was more efficient to torsional strength compared to the longitudinal CFRP wrap. The increase in the experimental ultimate load was (42%, 48% and 37%) for the beams with  $T/L$  equals (0.58, 0.15 and 0.095) respectively. The orientation angle of the vertical CFRP was ( $90^\circ$ ). The term  $(\sin\beta)$  is equal to (1) which means that the vertical position of the CFRP is better than the horizontal even the oblique. The comparison of the analytical and experimental results for beams without, with longitudinal and with transverse CFRP wrap are shown in Figs. 7 to 9 respectively. The experimental ultimate load was found larger than

the calculated load from the equations when the  $T/L$  ratio tends to a minimum, while the experimental load was found to be smaller when the  $T/L$  ratio tends to a maximum. The intersection points between the experimental and analytical bilinear lines represent the coinciding points of the  $T/L$  ratio, which is projected on the horizontal axis. The values calculated from the equations seem less conservative than the experimental values as the  $T/L$  ratio increases beyond the intersection points.

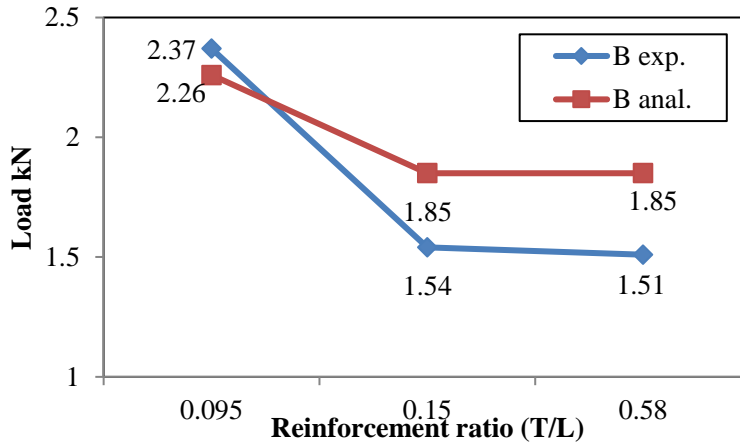


**Fig. 7. Experimental and analytical comparison for the beams without CFRP wrap.**

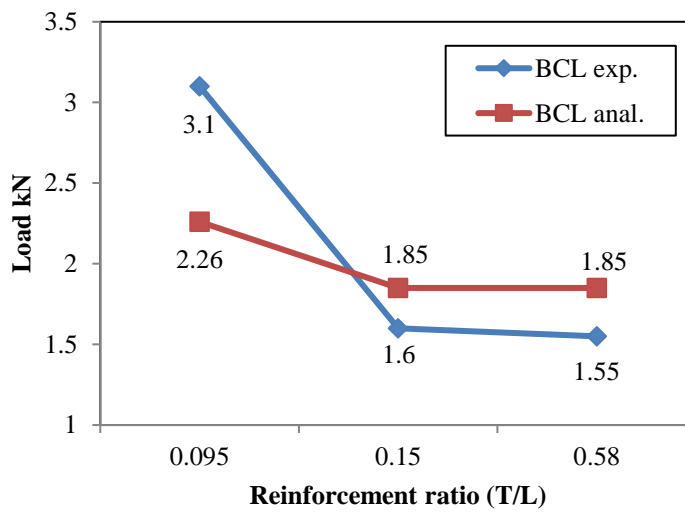


**Fig. 8. Experimental and analytical comparison for the beams with longitudinal CFRP wrap.**

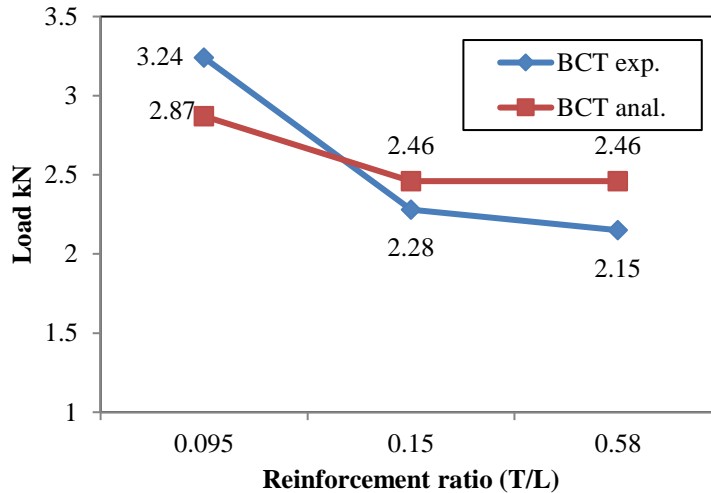


**Fig. 9. Experimental and analytical comparison for the beams with transverse CFRP wrap.**

## 6. Conclusion

The following conclusions can be reached from the experimental and analytical results:

- The transverse CFRP wrap has a significant effect on the experimental torsional strength than the longitudinal CFRP.
- The torsional strength of RPC edge beams was affected by a product of multiplying the areas of the longitudinal and transverse steel reinforcement with different ratios of  $T/L$  regardless of the presence of the CFRP wrap.
- From the analytical equations, the contribution of transverse CFRP was clear in improving the torsional and shear strengths only, while the longitudinal CFRP had no contribution in torsional, shear, and flexural strengths.
- Unlike the analytical results, the longitudinal CFRP wrap improved the experimental ultimate load and this improvement increased as the longitudinal reinforcement increased.
- Acceptable compatibility was found between the experimental and the theoretical results.
- In all beams, the failure mode occurred as a torsional failure mode which represents the lower value than the shear and flexural failure load. Therefore; it is important to give more attention to the torsion and flexural design than the shear design of RPC edge beams under this case of combined loading.
- Investigation of the contribution of the longitudinal CFRP in the torsional strength in addition to shear and flexural strengths separately is recommended as future work.

## Acknowledgment

The authors would like to thank the Mustansiriyah University ([www.uomustansiriyah.edu.iq](http://www.uomustansiriyah.edu.iq)) Baghdad-Iraq for its support in the present work.

**Nomenclatures**

$A_C$	Area enclosed within the outer perimeter of the cross-section
$A_L$	Total area of symmetrically distributed longitudinal reinforcement
$A_s$	Area of tension steel reinforcement;
$A_{sl}$	Total area of longitudinal reinforcement;
$A_{st}$	Total area of stirrups in 1000 mm long of beam
$A_t$	Area of the bar of hoop transverse reinforcement
$a$	Depth of stress block
$\underline{a}$	Shear span
$B_f$	Bond factor; taken as 0.5 for round fibres
$b_f$	Minimum width of the cross-section of CFRP
$b_w$	Width of the beam web
$c$	Neutral axis depth
$d$	Depth of tension steel (effective depth of the section)
$d_f$	Diameter of steel fibre
$E_f$	Modulus of elasticity of CFRP in the principal fibre orientation
$e$	Eccentricity of the applied load
$\underline{e}$	Distance from extreme compression fibre to top of tensile stress block of fibrous concrete
$F$	Fibre factor
$F_{be}$	Bond efficiency factor; taken as 1.0
$F_{theo}$	Nominal flexural load calculated from the theoretical equation
$f_y$	Yield strength of steel rebar
$f_{yt}$	Yield strength of hoop transverse reinforcement
$f_{yl}$	Yield strength of longitudinal reinforcement
$f'_c$	Specified compressive strength of concrete
$h$	Height of beam section
$l_f$	Length of steel fibre
$M_n$	Nominal flexural strength
$P_C$	Outer perimeter of the cross-section
$P_{uexp.}$	Measured failure load
$s$	Spacing of transverse reinforcement, parallel to the axis of the specimen
$s_f$	Centre to centre spacing of CFRP wrap
$S_{theo}$	Nominal shear load calculated from the theoretical equation
$T_n$	Calculated ultimate torsional moment
$T_{nfrp}$	Carbon fibre contribution in torsional moment
$T_{theo}$	Nominal torsional load calculated from the theoretical equation
$t_f$	Thickness of the CFRP sheet
$V_n$	Nominal shear strength
$v_f$	Volume fraction of steel fibres
$w_f$	Sheet width
$z_f$	The effective depth of CFRP

**Greek Symbols**

$\alpha$	Angle of torsion crack
----------	------------------------

$\beta$	Angle of orientation of the fibres from the member's longitudinal axis
$\varepsilon_{f k,e}$	Characteristic value of effective fibre strain
$\varepsilon_{sf}$	Strain in tension side of steel fibre
$\rho_f$	CFRP reinforcement ratio (percent by volume of steel fibre)
$\sigma_t$	Tensile strength of steel fibre reinforced concrete
<b>Abbreviations</b>	
ACI	American Code Institute
ASTM	American Society for Testing and Materials
CFRP	Carbon Fibre Reinforced Polymers
IOS	Iraqi Specifications
RPC	Reactive Powder Concrete

## References

1. Pham, H.; and Al-Mahaidi, R. (2004). Experimental investigation into flexural retrofitting of reinforced concrete bridge beams using FRP composites. *Composite Structures*, 66(1), 617-625.
2. El-Gamal, S.E.; Al-Nuaimi, A.; Al-Saidy, A.; and Al-Lawati, A. (2016). Efficiency of near surface mounted technique using fibre reinforced polymers for the flexural strengthening of RC beams. *Construction and Building Materials*, 118, 52-62.
3. Raoof, S.M.; Koutas, L.N.; and Bournas, D.A. (2017). Textile-reinforced mortar (TRM) versus fibre-reinforced polymers (FRP) in flexural strengthening of RC beams. *Construction and Building Materials*, 151, 279-291.
4. Tanarslan, H.M. (2017). Flexural strengthening of RC beams with prefabricated ultra-high performance fibre reinforced concrete laminates. *Engineering Structures*, 151, 337-348.
5. Tanarslan, H.M.; Alver, N.; Jahangiri, R.; Yalçinkaya, Ç.; and Yazıcı, H. (2017). Flexural strengthening of RC beams using UHPFRC laminates: Bonding techniques and rebar addition. *Construction and Building Materials*, 155, 45-55.
6. Yang, X.; Gao, W.Y.; Dai, J.G.; Lu, Z.D.; and Yu, K.Q. (2018). Flexural strengthening of RC beams with CFRP grid-reinforced ECC matrix. *Composite Structures*, 189, 9-26.
7. Pellegrino, C.; and Modena, C. (2002). Fibre reinforced polymer shear strengthening of reinforced concrete beams with transverse steel reinforcement. *Journal of Composites for Construction*, 6(2), 104-111.
8. Zhang, Z.; and Hsu, C.T. (2005). Shear strengthening of reinforced concrete beams using carbon-fibre-reinforced polymer laminates. *Journal of Composites for Construction*, 9(2), 158-169.
9. Monti, G.; and Liotta, M.A. (2007). Tests and design equations for FRP-strengthening in shear. *Construction and Building Materials*, 21(4), 799-809.
10. Abdalla, J.A.; Abu-Obeidah, A.S.; Hawileh, R.A.; and Rasheed, H.A. (2016). Shear strengthening of reinforced concrete beams using externally-bonded aluminum alloy plates: An experimental study. *Construction and Building Materials*, 128, 24-37.

11. Younis, A.; Ebead, U.; and Shrestha, K.C. (2017). Different FRCC systems for shear-strengthening of reinforced concrete beams. *Construction and Building Materials*, 153, 514-526.
12. Wakjira, T.G.; and Ebead, U. (2018). Hybrid NSE/EB technique for shear strengthening of reinforced concrete beams using FRCC: Experimental study. *Construction and Building Materials*, 164, 164–177.
13. Marcinczak, D.; Trapko, T.; and Musiał, M. (2019). Shear strengthening of reinforced concrete beams with PBO-FRCC composites with anchorage. *Composites Part B: Engineering*, 158, 149-161.
14. Greene, J.G.; and Belarbi, A. (2009). Model for Reinforced Concrete Members under torsion, bending, and shear. I: Theory. *Journal of Engineering Mechanics*, 135(9), 961-969.
15. Breveglieri, M.; Aprile, A.; and Barros, J.A.O. (2016). RC beams strengthened in shear using the Embedded Through-Section technique: Experimental results and analytical formulation. *Composites Part B: Engineering*, 89, 266-281.
16. Al-Osta, M.A.; Isa, M.N.; Baluch, M.H.; and Rahman, M.K. (2017). Flexural behavior of reinforced concrete beams strengthened with ultra-high performance fibre reinforced concrete. *Construction and Building Materials*, 134, 279-296.
17. Alabdulhady, M.Y.; and Sneed, L.H. (2017). Torsional strengthening of reinforced concrete beams with externally bonded composites: A state of the art review. *Construction and Building Materials*, 205, 148-163.
18. Wakjira, T.G.; and Ebead, U. (2019). Experimental and analytical study on strengthening of reinforced concrete T-beams in shear using steel reinforced grout (SRG). *Composites Part B: Engineering*, 177, 107368.
19. Nawaz, W.; Hawileh, R.A.; Saqan, E.I.; and Abdalla, J.A. (2016). Effect of longitudinal carbon fibre-reinforced polymer plates on shear strength of reinforced concrete beams. *ACI Structural Journal*, 113(3), 577-686.
20. Adam, V.; Herbrand, M.; and Hegger, J. (2017). Shear and flexural strengthening of existing bridges with textile reinforced mortar. 39<sup>th</sup> IABSE Symposium. Vancouver, Canada, 2496-2503.
21. Chennareddy, R.; and Taha, M.M.R. (2017). Effect of combining near-surface-mounted and U-wrap fibre-reinforced polymer strengthening techniques on behavior of reinforced concrete beams. *ACI Structural Journal*, 114(3), 719-728.
22. Ferdous, W.; Manalo, A.; Aravinthan, T.; and Fam, A. (2018). Flexural and shear behaviour of layered sandwich beams. *Construction and Building Materials*, 173, 429–442.
23. Herbrand, M.; Adam, V.; and Hegger, J. (2018). Investigations on the Strengthening of Existing Highway Bridges Under Shear and Flexural Loading with Textile Reinforced Mortar. *Proceedings of the 2017 fib Symposium*. Maastricht, Netherlands, 1959-1967.
24. Lee, J.K.; and Jeong, S. (2016). Flexural and torsional free vibrations of horizontally curved beams on Pasternak foundations. *Applied Mathematical Modelling*, 40(3), 2242-2256.
25. Machado-e-Costa, M.; Valarinho, L.; Silvestre, N.; and Correia, J.R. (2016). Modeling of the structural behavior of multilayer laminated glass beams:

- Flexural and torsional stiffness and lateral-torsional buckling. *Engineering Structures*, 128, 265-282.
26. Nguyen, T.-T.; Thang, P.T.; and Lee, J. (2017). Flexural-torsional stability of thin-walled functionally graded open-section beams. *Thin-Walled Structures*, 110, 88-96.
  27. Patel, P.V.; Jariwala, V.H.; and Purohit, S.P. (2016). Torsional strengthening of RC beams using GFRP composites. *Journal of The Institution of Engineers (India): Series A*, 97(3), 313-322.
  28. Al-Bayati, G.; Al-Mahaidi, R.; and Kalfat, R. (2017). Torsional strengthening of reinforced concrete beams using different configurations of NSM FRP with epoxy resins and cement-based adhesives. *Composite Structures*, 168, 569-581.
  29. Al-Bayati, G.; Al-Mahaidi, R.; Hashemi, M.J.; and Kalfat, R. (2018). Torsional strengthening of RC beams using NSM CFRP rope and innovative adhesives. *Composite Structures*, 187, 190-202.
  30. Triantafyllou, T.C.; and Antonopoulos, C.P. (2000). Design of concrete flexural members strengthened in shear with FRP. *Journal of Composites for Construction*, 4(4), 198-205.
  31. Sure, N. (2013). *Experimental and analytical study on torsional behavior of RC flanged beams strengthened with glass FRP*. M.Sc. Dissertation; National Institute of Technology, Odisha, India.
  32. Dong, J.; Wang, Q.; and Guan, Z. (2013). Structural behavior of RC beams with external flexural and flexural-shear strengthening by FRP sheets. *Composites Part B: Engineering*, 44(1), 604-612.
  33. Mahmood, M.N.; and Mahmood, A.S. (2011). Torsional behavior of prestressed concrete beams strengthened with CFRP sheets. *16th International Conference on Composite Structures ICCS*. Porto, Portugal, 1-12.
  34. Mohammad, K.I.; and Al-Sulayfani, B.J.; (2012). An investigation on torsional behaviour of RC beams strengthened with CFRP. *10th International Congress on Advances in Civil Engineering*. Ankara, Turkey, 1-9.
  35. Zhang, J.W.; Lu, Z.T.; and Zhu, H. (2001). Experimental study on the behavior of RC torsional members externally bonded with CFRP. *In Proceeding International Conference on FRP Composites in Civil Engineering*. Hong Kong, China, 713-722.
  36. Ghorbarah, A.; Ghorbel, M.; and Chidiac, S. (2002). Upgrading torsional resistance of reinforced concrete beams using fibre-reinforced polymer. *Journal of Composites for Construction*, 6(4), 257-263.
  37. Hii, A.K.Y.; and Al-Mahaidi, R. (2007). Torsional capacity of CFRP strengthened reinforced concrete beams. *Journal of Composites for Construction*, 11(1), 71-80.
  38. Ameli, M.; and Ronagh, H.R. (2007). Analytical method for evaluating ultimate torque of FRP strengthened reinforced concrete beams. *Journal of Composites for Construction*, 11(4), 384-390.
  39. Kwahk, I.; Joh, Ch.; and Lee, J.W. (2015). Torsional behavior design of UHPC box beams based on thin-walled tube theory. *Engineering*, 7, 101-114.
  40. Iraqi Specifications No. 5 (1984). *Portland Cement*. Ministry of Planning, Central Organization for Standardization and Quality Control. Baghdad, IRAQ.



41. Iraqi Specification, No. 45 (1984). *Aggregate from Natural Sources for Concrete and Construction*. Ministry of Planning, Central Organization for Standardization and Quality Control. Baghdad, IRAQ.
42. ASTM C1240 (2020). *Standard Specification for Silica Fume Used in Cementitious Mixtures*. West Conshohocken, PA, USA.
43. ASTM C39 / C39M (2018). *Standard Test Method for Compressive Strength of Cylindrical Concrete Specimens*. West Conshohocken, PA, USA.
44. ASTM C496 / C496M (2017). *Standard Test Method for Splitting Tensile Strength of Cylindrical Concrete Specimens*. West Conshohocken, PA, USA.
45. ASTM C78 / C78M (2018). *Standard Test Method for Flexural Strength of Concrete (Using Simple Beam with Third-Point Loading)*. West Conshohocken, PA, USA.
46. ASTM C469 / C469M (2014). *Standard Test Method for Static Modulus of Elasticity and Poisson's Ratio of Concrete in Compression*. West Conshohocken, PA, USA.
47. Rahal, Kh.N. (2013). Torsional strength of normal and high strength reinforced concrete beams. *Engineering Structures*, 56, 2206-2216.
48. Mohammadizadeh, M.R.; and Fadaee, M.J. (2009). Torsional behavior of high strength concrete beams strengthened using CFRP sheets; an experimental and analytical study. *Civil Engineering, Sharif University of Technology*, 16(4), 321-330.
49. ACI Committee 440.2R. (2017). *Guide for the Design and Construction of Externally Bonded FRP Systems for Strengthening Concrete Structures*. Farmington Hills, USA.
50. Ashour, S.A.; Hasanain, G.S.; and Wafa, F.F. (1992). Shear behavior of high-strength fibre reinforced concrete beams. *ACI Structural Journal*, 89(2), 176-184.
51. ACI Committee 544 (1988). Design considerations for steel fibre reinforced concrete. *International Concrete Abstracts Portal*, 85(5), 563-579.